

# NUMERICAL MODEL FOR CALCULATION OF HYDRAULIC TRANSIENT AND FLUID-STRUCTURE INTERACTION IN FLUID TRANSPORT SYSTEMS

Rafael S.P. Almeida<sup>1</sup> and Marcelo S. Rocha<sup>1</sup>

<sup>1</sup> Instituto de Pesquisas Energéticas e Nucleares (IPEN / CNEN - SP)  
Av. Professor Lineu Prestes 2242  
05508-000 São Paulo, SP, Brazil  
[rafael.almeida@ipen.br](mailto:rafael.almeida@ipen.br)  
[msrocha@ipen.br](mailto:msrocha@ipen.br)

## ABSTRACT

In this study the effects of Fluid-structure Interaction during hydraulic transients, more precisely water hammer events, in fluid transport systems are investigated. For this purpose, a numerical model was developed to simulate the effects of Fluid-structure Interaction in a system composed of a reservoir with upstream constant level, a straight pipe and a valve coupled downstream, which can be rigidly fixed or free to move. The transfer of energy from the fluid to the structure associated with pressure waves and their effects, that is, the efforts and displacements generated, is taken into account. The Method of Characteristics is used for solving the hyperbolic partial differential equations system, associated with finite differences and linear interpolations procedures. Three coupling mechanisms are modeled: Friction, Poisson, and junction coupling. The proposed numerical procedure is validated by simulation of a benchmark problem and compared to analytical solutions found in the literature. The results indicated that the model is able to reproduce the main effects of Fluid-structure Interaction during hydraulic transients in a pipe conveying fluids.

### List of symbols

A - cross-sectional area, m <sup>2</sup>	MOC - Method of Characteristics
c - classical wave speed, celerity, m/s	P - pressure, Pa
$c^*$ - FSI wave speed, celerity, m/s	R - inner radius of pipe, m
D - inner diameter of pipe, m	T - period, s
E - Young modulus of pipe wall, Pa	t - time, s
e - pipe wall thickness, m	u - pipe displacement, m
FSI - Fluid-Structure Interaction	$\dot{u}$ - pipe velocity, m/s
G - shear modulus of pipe wall material, Pa	V - cross-sectional fluid velocity, m/s
H - pressure head, m	x - axial coordinate, m
K - fluid bulk modulus, Pa	g - constant, m/s
L - length, m	$\mu$ - Poisson ratio

## 1. INTRODUCTION

Fluid transport systems are widely used in many fields of engineering such as nuclear and electric power industries, petroleum and chemical process industries, Water supply systems and in many other applications. Those systems are often subject to large pressure fluctuations due to, for example, the rapid closing or opening of valves, or to the stopping or starting of pumps. This phenomenon is called hydraulic transients, being the worst scenario a water hammer event, when great magnitude pressure surge may occur [1], [2], [3].

The classical water hammer theory [4] is accurate to predict extreme loadings on a system, only if it is rigidly anchored. When a piping system has certain degrees of freedom, severe deviations from classical theory may occur due to motion of the system [1], [5], [6]. Motion of the system causes the fluid to interact with pipe structure. That interaction highly influences the extreme pressures during water hammer occurrences.

To accurately predict hydrodynamic loads in the fluid, as well as pipe stress and vibrations, the analyses of fluid and pipe movements must be conducted simultaneously in a coupled manner. This approach is referred in the literature as Fluid-structure Interaction (FSI) [5], [6]. FSI has been the subject of intense research in recent years. Excellent review work may be found in [2], [3], [7], [8], [9].

Fluid-structure Interaction deals with the transfer of momentum and forces between a pipeline and its contained fluid. In this case, interaction mechanisms have to be taken into account. Three interaction (coupling) mechanisms occur during FSI in straight pipes [1], [3],[5]: Friction coupling is due to friction between pipe wall and the fluid; Poisson coupling relates the pressures in the fluid to the axial stresses in the pipe via the contraction or expansion of the pipe wall; Junction coupling takes place at pipe boundaries that can move, either in response to changes in fluid pressure or because of external excitation [5],[10].

In some cases, FSI may be responsible for engineering critical operational behavior (vibrations, oscillations, etc.), or even failure of the tube or its entire system. When the safety of the system in question is very critical such as, for example, nuclear power plants, which are subjected to extreme conditions of pressure and temperature, it is significant to know the exact operating conditions during transients and, for this reason, it is very important the development specific computational codes to do so.

The main goal of this work is to develop a computational tool, based on the four equation model [1],[2],[6] to simulate the effects of FSI during water hammer events in filled straight pipes conveying fluid.

State of art FSI codes takes into account torsional, lateral and axial motion, as well as the effects of pipe wall radial stress and displacement [9],[11]. Generally the fourteen equation model is solved. More complex systems of fluid-filled pipes with straight, curved and branch pipes may be analyzed.

## 2. BASIC EQUATIONS AND ASSUMPTIONS

In the analysis of the hydraulic transients and FSI, it is desired to determine the fluid pressure  $P$  (or pressure head  $H$ ), fluid velocities  $V$  (or flow rates  $Q$ ), pipe axial stresses  $\sigma$  and axial pipe velocities  $\dot{u}$ , as a function of position ( $x$ ) and time ( $t$ ), that is,  $P(x,t)$ ,  $V(x,t)$ ,  $\sigma(x,t)$  and  $\dot{u}(x,t)$ .

Longitudinal pressure waves are essentially the relevant hydrodynamic loads in an FSI model. These models are described by partial hyperbolic differential equations. Two equations for the liquid are coupled to two equations for the pipe [3].

Assumptions: the pipe is straight, prismatic, of circular cross-section, slender and thin-walled. The liquid and the pipe-wall material are assumed linearly elastic. For the fluid it is assumed that the long wave length and the acoustic approximation are valid.

### 2.1 Equations for the fluid

The equations for momentum and continuity are applied to the mean flow. Two equations for fluid velocity ( $V$ ) and fluid pressure head ( $H$ ) are provided by the momentum balance and the mass balance [2].

$$\frac{\partial V}{\partial t} + g \frac{\partial H}{\partial x} = -f \frac{V_{\text{rel}} |V_{\text{rel}}|}{4R} \quad (1)$$

$$\frac{\partial V}{\partial x} + \frac{g}{a_f^2} \frac{\partial H}{\partial t} = 2\mu \frac{\partial \dot{u}_x}{\partial x} \quad (2)$$

In which

$$a_f = \sqrt{\frac{K_f}{\rho_f \left(1 + \frac{CK_f D}{eE}\right)}} \quad (3)$$

$$V_{\text{rel}} = V - \dot{u}_x \quad (4)$$

Equations (1) and (2) describe the propagation of pressure waves under the influence of axial pipe vibrations and govern the unknowns of fluid pressure, fluid velocity, and axial pipe velocity ( $\dot{u}_x$ ).

### 2.2 Equations for pipe axial motion

The governing equations for the axial motion of the pipe are provided by the momentum balance and the stress-strain relation. The pipe is described by its axial velocity ( $\dot{u}_x$ ) and axial stress ( $\sigma_x$ ) [6].

$$\frac{\partial \dot{u}_x}{\partial t} - \frac{1}{\rho_t} \frac{\partial \sigma_x}{\partial x} = f \frac{\rho_f A_f V_{rel} |V_{rel}|}{\rho_t A_t 4R} + g \sin \theta \quad (5)$$

$$\frac{\partial \dot{u}_x}{\partial x} - \frac{1}{\rho_t a_t^2} \frac{\partial \sigma_x}{\partial t} = -\rho_f g \frac{\mu R}{E_e} \frac{\partial H}{\partial t} \quad (6)$$

In which

$$a_t = \sqrt{\frac{E}{\rho_t}} \quad (7)$$

Equations (1) and (5) are coupled via terms proportional to Poisson's ratio. These terms represent the Poisson coupling. Equations (2) and (6) are coupled via terms proportional to the friction coefficient,  $f$ . These terms govern the friction coupling. Junction coupling is a result of local forces and therefore modelled via boundary conditions [6]. The friction is modelled as if the flow were steady.

The Four equation model is presented. It consists of a system of hyperbolic partial differential equations that simultaneously describe the propagation of pressure waves in the liquid and axial stress waves in the pipe. Due to its hyperbolic character, the system can be converted to a set of four ordinary differential equations by the MOC transformation [10].

## 2.3 Initial and boundary conditions

### 2.3.1 Boundary Conditions

Reservoir – the reservoir is considered to have constant level with a pipe rigidly connected to it:

$$H(0, t) = H_U \quad (8)$$

$$\dot{u}(0, t) = 0 \quad (9)$$

Valve - the valve is modelled as being rigidly fixed or free to move axially. The following relationships satisfy these conditions:

- a) instantaneous closure of a valve rigidly fixed to the ground:

$$V(x = L, t) = 0 \quad (10)$$

$$\dot{u}(x = L, t) = 0 \quad (11)$$

- b) instantaneous closure of a valve free to move axially:

$$V(x = L, t) = \dot{u}(x = L, t) \quad (12)$$

$$\rho_f \cdot g \cdot A_f \cdot \Delta H = A_t \cdot \Delta \sigma_x \quad (13)$$

- c) noninstantaneous closure of a valve, equations (10) and (12) are replaced by:

$$\Delta H = H_D + K_v \frac{V_{rel}|V_{rel}|}{2g} \quad (14)$$

In which  $K_v$  is the load loss coefficient in the valve and  $C_d$  is the valve discharge coefficient [4]:

$$K_v = \frac{1}{C_d^2} - 1 \quad (15)$$

### 2.3.2 Initial Conditions

The initial conditions are the steady-state conditions just before the hydraulic transient.

$$H(x, 0) = H_U - \left[ \rho_f f \frac{V_{rel}|V_{rel}|}{4R} - \rho_f \cdot g \cdot \text{sen}\theta \right] x \quad (16)$$

$$V(x, 0) = \text{constant} \quad (17)$$

$$\sigma(x, 0) = \sigma(0,0) - \left[ \frac{1}{\left(1 + \frac{1}{2R}\right)e} \rho_f f \frac{V_{rel}|V_{rel}|}{4R} \rho_t \cdot g \cdot \text{sen}\theta \right] x \quad (18)$$

$$\dot{u}(x, 0) = 0 \quad (19)$$

## 3. NUMERICAL SOLUTION AND RESULTS

### 3.1 Numerical Solution

Equations (1), (2), (4) and (5) form a pair of hyperbolic equations of partial derivatives. Method of the Characteristics (MOC) [10] transforms these equations into total differential equations.

The MOC is a powerful method to deal with wave phenomena. With respect to water hammer the method has many advantages: stability is firmly established, boundary conditions can be programmed easily, and complex systems can be handled [1].

After MOC procedure, the so called equations of compatibility [1] [6] are obtained.

Fluid:

$$\begin{aligned} \frac{dV}{dt} + \frac{g}{a_f} \left[ \frac{\bar{a}_f}{a_f} + 2\mu^2 \frac{R \rho_f}{e \rho_t} \frac{\frac{a_f \bar{a}_f}{a_t^2}}{1 - \left(\frac{\bar{a}_f}{a_t}\right)^2} \right] \frac{dH}{dt} + 2\mu \frac{\left(\frac{\bar{a}_f}{a_t}\right)^2}{1 - \left(\frac{\bar{a}_f}{a_t}\right)^2} \frac{d\dot{u}_x}{dt} - \frac{2\mu}{\rho_t \bar{a}_f} \frac{\left(\frac{\bar{a}_f}{a_t}\right)^2}{1 - \left(\frac{\bar{a}_f}{a_t}\right)^2} \frac{d\sigma_x}{dt} = \\ = -f \frac{V_{rel}|V_{rel}|}{4R} + 2\mu \frac{\left(\frac{\bar{a}_f}{a_t}\right)^2}{1 - \left(\frac{\bar{a}_f}{a_t}\right)^2} \left[ f \frac{\rho_f A_f}{\rho_t A_t} \frac{V_{rel}|V_{rel}|}{4R} + g \cdot \text{sen}\theta \right] \end{aligned} \quad (20)$$

$$\begin{aligned} \frac{dV}{dt} - \frac{g}{a_f} \left[ \frac{\bar{a}_f}{a_f} + 2\mu^2 \frac{R \rho_f}{e \rho_t} \frac{\frac{a_f \bar{a}_f}{a_t^2}}{1 - \left(\frac{a_f}{a_t}\right)^2} \right] \frac{dH}{dt} + 2\mu \frac{\left(\frac{\bar{a}_f}{a_t}\right)^2}{1 - \left(\frac{a_f}{a_t}\right)^2} \frac{d\dot{u}_x}{dt} - \frac{2\mu}{\rho_t \bar{a}_f} \frac{\left(\frac{a_f}{a_t}\right)^2}{1 - \left(\frac{a_f}{a_t}\right)^2} \frac{d\sigma_x}{dt} = \\ = -f \frac{V_{rel}|V_{rel}|}{4R} + 2\mu \frac{\left(\frac{\bar{a}_f}{a_t}\right)^2}{1 - \left(\frac{a_f}{a_t}\right)^2} \left[ f \frac{\rho_f A_f V_{rel}|V_{rel}|}{\rho_t A_t 4R} + g \cdot \text{sen}\theta \right] \end{aligned} \quad (21)$$

Pipe:

$$\begin{aligned} -\mu \frac{R \rho_f}{e \rho_t} \frac{\left(\frac{a_f}{a_t}\right)^2}{1 - \left(\frac{a_f}{a_t}\right)^2} \frac{dV}{dt} - \mu \frac{R \rho_f}{e \rho_t} \frac{g \bar{a}_t}{a_t a_t} \frac{\left(\frac{a_f}{a_t}\right)^2}{1 - \left(\frac{a_f}{a_t}\right)^2} \frac{dH}{dt} + \left[ 1 + 2\mu^2 \frac{R \rho_f}{e \rho_t} \frac{\left(\frac{a_f}{a_t}\right)^2}{1 - \left(\frac{a_f}{a_t}\right)^2} \right] \frac{d\dot{u}_x}{dt} \\ - \frac{1}{\rho_t a_t} \frac{d\sigma_x}{dt} = \left[ 1 + 2\mu^2 \frac{R \rho_f}{e \rho_t} \frac{\left(\frac{a_f}{a_t}\right)^2}{1 - \left(\frac{a_f}{a_t}\right)^2} \right] \left[ f \frac{\rho_f A_f V_{rel}|V_{rel}|}{\rho_t A_t 4R} + g \cdot \text{sen}\theta \right] + \\ \mu \frac{R \rho_f}{e \rho_t} \frac{\left(\frac{a_f}{a_t}\right)^2}{1 - \left(\frac{a_f}{a_t}\right)^2} f \frac{V_{rel}|V_{rel}|}{4R} \end{aligned} \quad (22)$$

$$\begin{aligned} -\mu \frac{R \rho_f}{e \rho_t} \frac{\left(\frac{a_f}{a_t}\right)^2}{1 - \left(\frac{a_f}{a_t}\right)^2} \frac{dV}{dt} + \mu \frac{R \rho_f}{e \rho_t} \frac{g \bar{a}_t}{a_t a_t} \frac{\left(\frac{a_f}{a_t}\right)^2}{1 - \left(\frac{a_f}{a_t}\right)^2} \frac{dH}{dt} + \left[ 1 + 2\mu^2 \frac{R \rho_f}{e \rho_t} \frac{\left(\frac{a_f}{a_t}\right)^2}{1 - \left(\frac{a_f}{a_t}\right)^2} \right] \frac{d\dot{u}_x}{dt} \\ + \frac{1}{\rho_t a_t} \frac{d\sigma_x}{dt} = \left[ 1 + 2\mu^2 \frac{R \rho_f}{e \rho_t} \frac{\left(\frac{a_f}{a_t}\right)^2}{1 - \left(\frac{a_f}{a_t}\right)^2} \right] \left[ f \frac{\rho_f A_f V_{rel}|V_{rel}|}{\rho_t A_t 4R} + g \cdot \text{sen}\theta \right] + \\ \mu \frac{R \rho_f}{e \rho_t} \frac{\left(\frac{a_f}{a_t}\right)^2}{1 - \left(\frac{a_f}{a_t}\right)^2} f \frac{V_{rel}|V_{rel}|}{4R} \end{aligned} \quad (23)$$

In which  $\bar{a}_f$  and  $\bar{a}_t$  are the adjusted values for the celerity of fluid and stress waves respectively:

$$\bar{a}_f = \left\{ 0.5 \left[ q^2 - (q^4 - 4a_f^2 a_t^2)^{\frac{1}{2}} \right]^{\frac{1}{2}} \right\} \quad (24)$$

$$\bar{a}_t = \{0.5 [q^2 + (q^4 - 4a_f^2 a_t^2)^{\frac{1}{2}}]\}^{\frac{1}{2}} \quad (25)$$

$$q = \sqrt{a_f^2 + a_t^2 + 2\mu^2 \frac{R \rho_f}{e \rho_t} a_f^2} \quad (26)$$

The following characteristic lines complete the system, respectively for equations:

$$+\bar{a}_f, -\bar{a}_f, +\bar{a}_t \text{ e } -\bar{a}_t \quad (27)$$

The compatibility equations (20)-(23) can now be easily integrated. The left-hand sides are integrated exactly, the nonlinear right-hand sides numerically [1],[2]. The integrations take place on a computational grid, which is based on the characteristic lines along which the pressure waves propagate, as shown in Figure 1. The mesh spacings  $\Delta x$  and  $\Delta t$  are constant. In this grid the points A1 and A2 are grid points. Points A3 and A4 fall between two grid points. In this cases interpolations are necessary.

The ultimate result is to determine the variables of interest (P, V,  $\sigma$  and  $\dot{u}$ ), at any point, P, in the interior (z, t)-plane, expressed in its values at four former points, A1, A2, A3, A4.

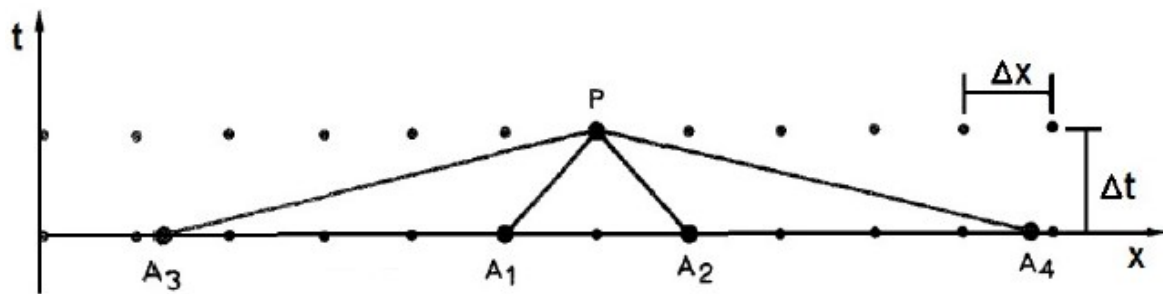


**Figure 1 - Time X space plan. Characteristic lines feedind point “P” to determine the unknowns.**

Interpolations are necessary when numerical data is required in between grid points (A3, A4). The distance–time plane is covered with rectangular mesh spacing.

The standard approach is to cover the distance–time plane with equidistantly spaced grid-points and to time-march from a given initial state [1],[6].

The formulation presented gather conditions to create a numerical procedure. A computational code, named FSI\_01, was developed.

### 3.2 Results

The methodology used to validate FSI\_01 code was to compare the results obtained with those of existing analytical solutions in the literature. For that, data from the exact solution presented by Tijsseling [6], who kindly yielded the files of the answers obtained for the Delft Benchmark problem "A", were used. It is assumed that the valve is free to move in the axial direction and has negligible mass. It is considered instant closure of the valve.

The Delft Hydraulics Benchmark Problems (A to F) have been defined and used to test numerical methods and FSI software [6]. It is noted that the benchmark problems are numerical test cases only; experimental data does not exist. Problem A concerns a reservoir-pipe valve system defined by Figure 2. The characteristics of the test case are resumed in Table 1.

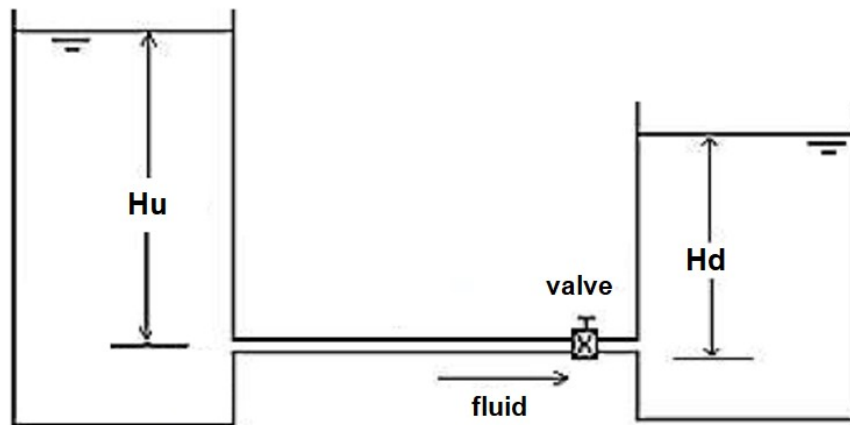


**Figure 2 - Reservoir pipe valve system**

**Table 1 - Delft Hydraulics Benchmark Problem A**

L	20	m
$\mu$	0.3	-
D	0,798	m
f	0,02	-
e	0,008	m
Tc	0	s
tmax	0,10	s
V	1	m/s
Hd	0	m
VOi	100	%

Figures 3 to 5 validate results of FSI\_01 against exactly solution [6] for Delft Hydraulics Benchmark Problem A. Fluid pressure, pipe wall stress and Fluid Velocity are calculated at valve section. The agreement between exactly solution and FSI\_01 calculation is excellent.

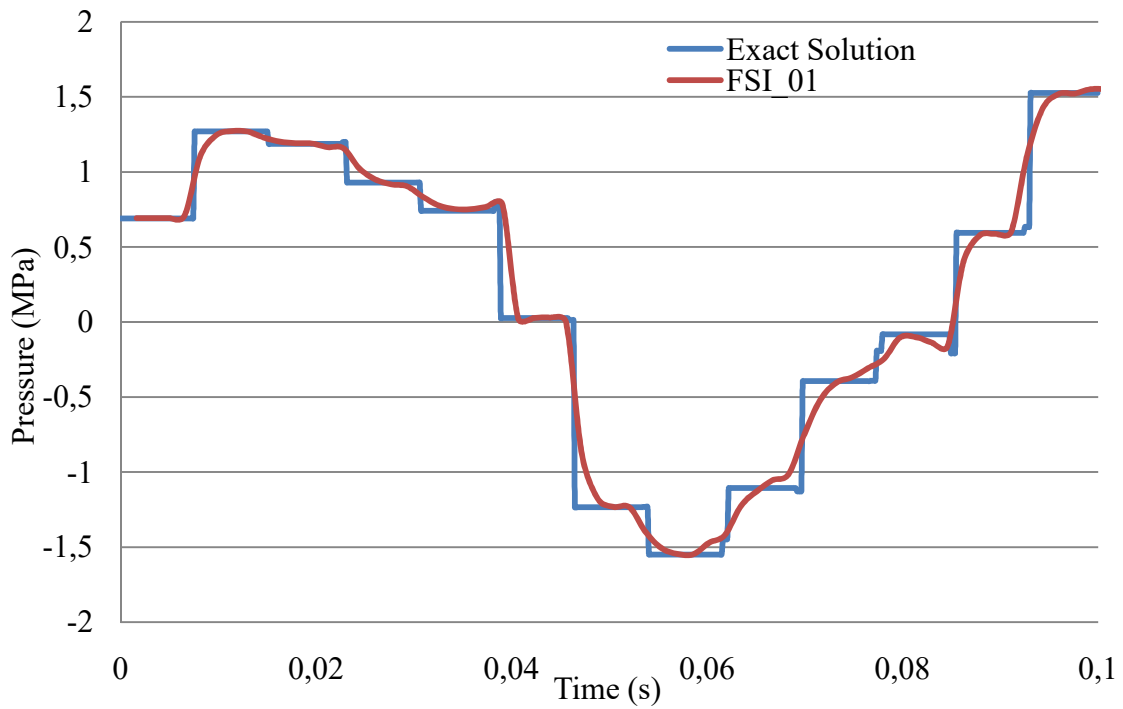


**Figure 3 - Validating results against exactly solution. Pressure at valve section for Delft Hydraulics Benchmark Problem A. Valve free to move.  $T_c=0$ .**

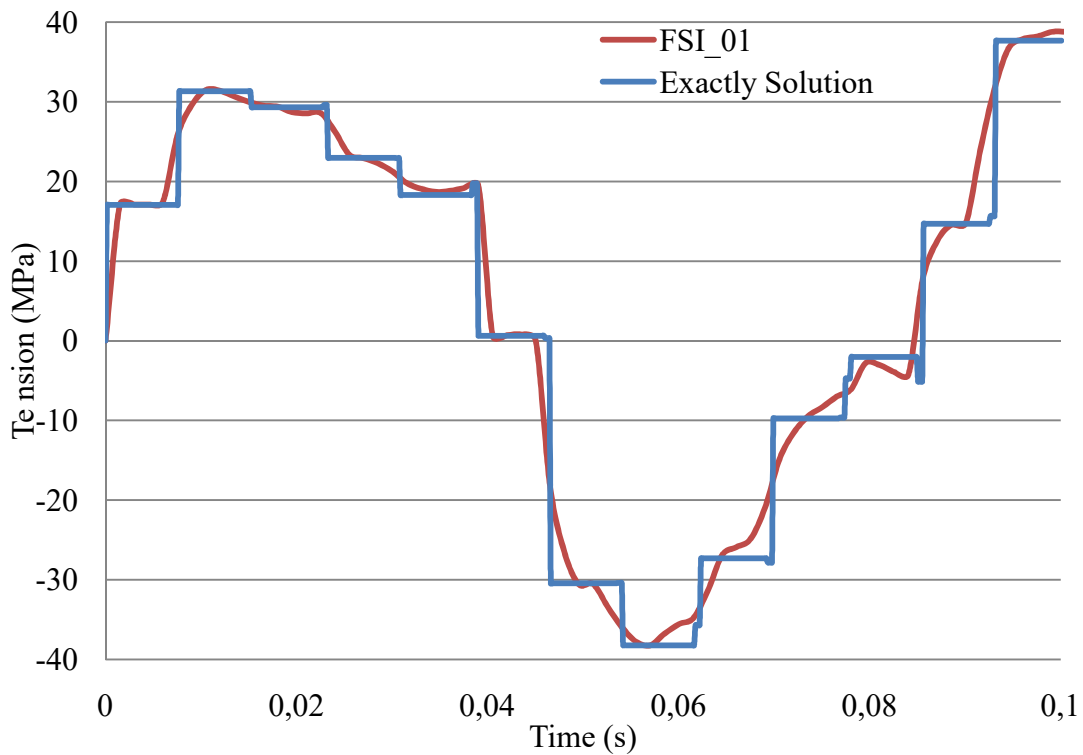


**Figure 4 - Validating results against exactly solution. Pipe axial Tension at valve section. for Delft Hydraulics Benchmark Problem A. Valve free to move.  $T_c=0$ .**

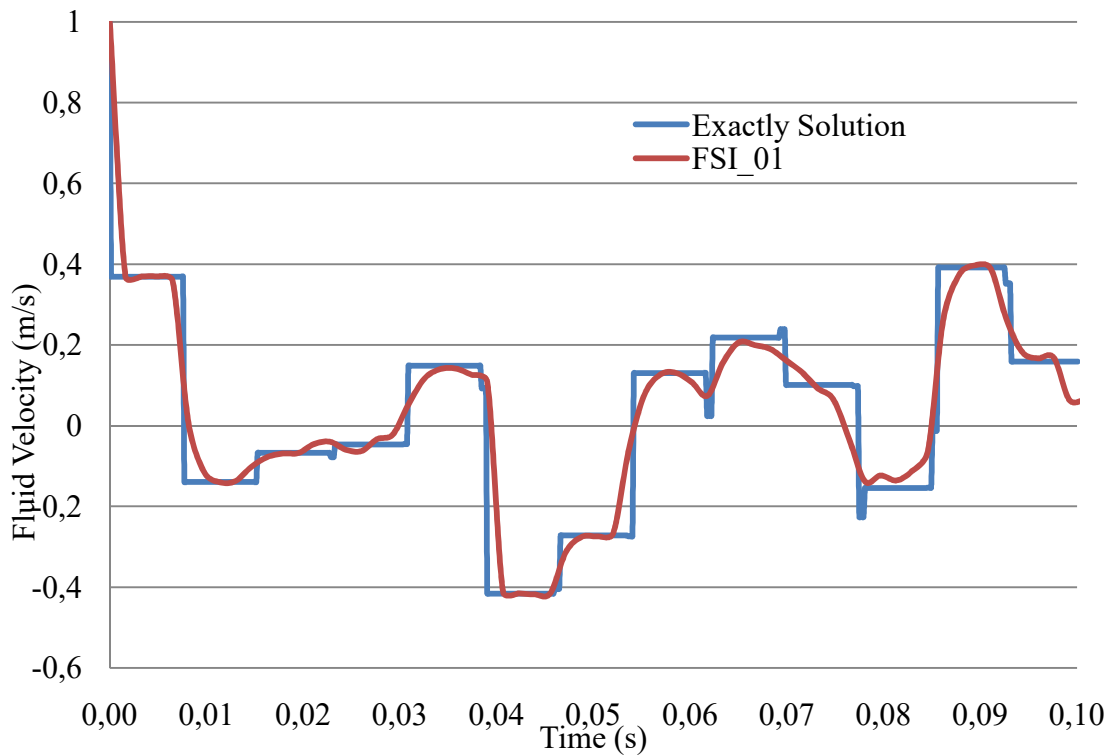


**Figure 5 - Validating results against exactly solution. Fluid velocity at valve section for Delft Hydraulics Benchmark Problem A. Valve free to move.  $T_c=0$ .**

Figures 6 to 8 show other comparison of classic water hammer result (no FSI) against Poisson coupling and Poisson and Junction coupling results.

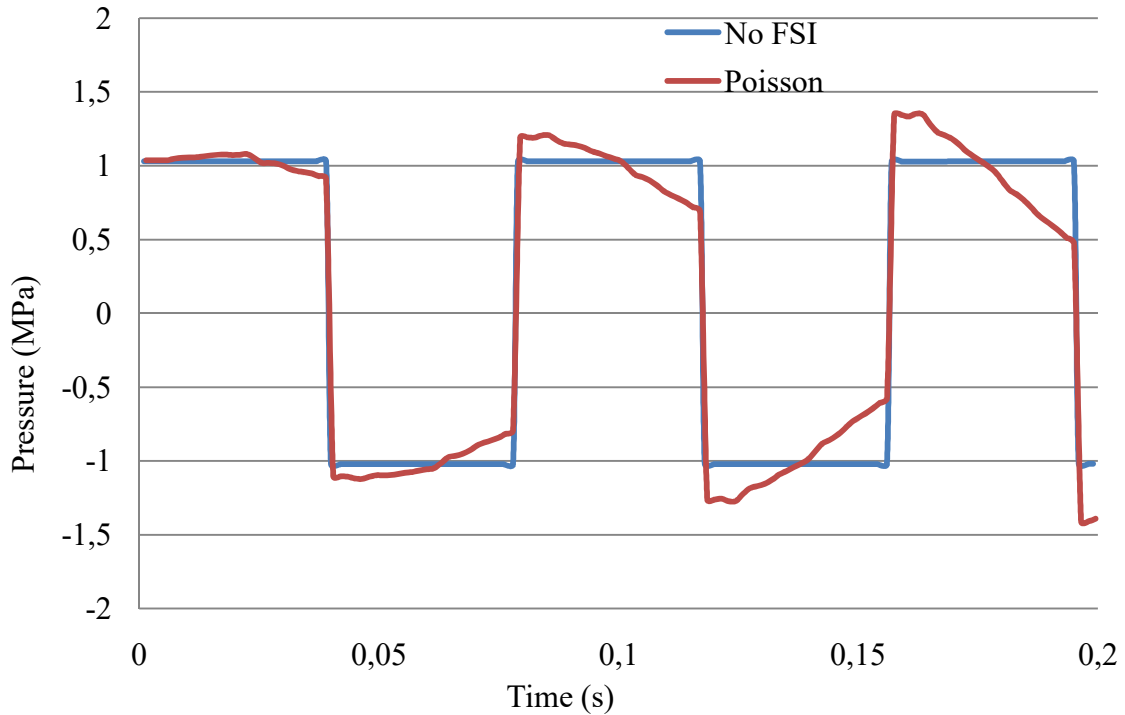


**Figure 6 – Comparison of classic water hammer result vs Poisson coupling. Pressure at valve for Delft Hydraulics Benchmark Problem A. Valve free to move.  $T_c=0$ .**

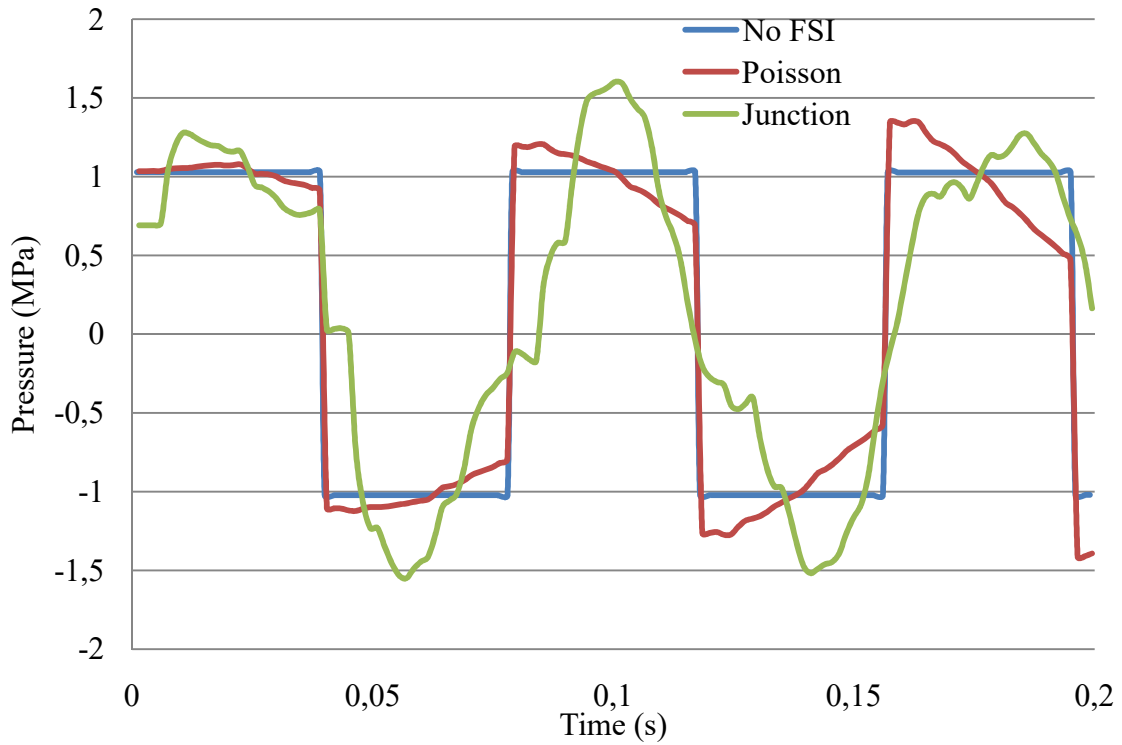


**Figure 7 – Comparison of classic water hammer result vs Poisson coupling vs Poisson and junction coupling. Pressure at valve for Delft Hydraulics Benchmark Problem A. Valve free to move.  $T_c=0$ .**

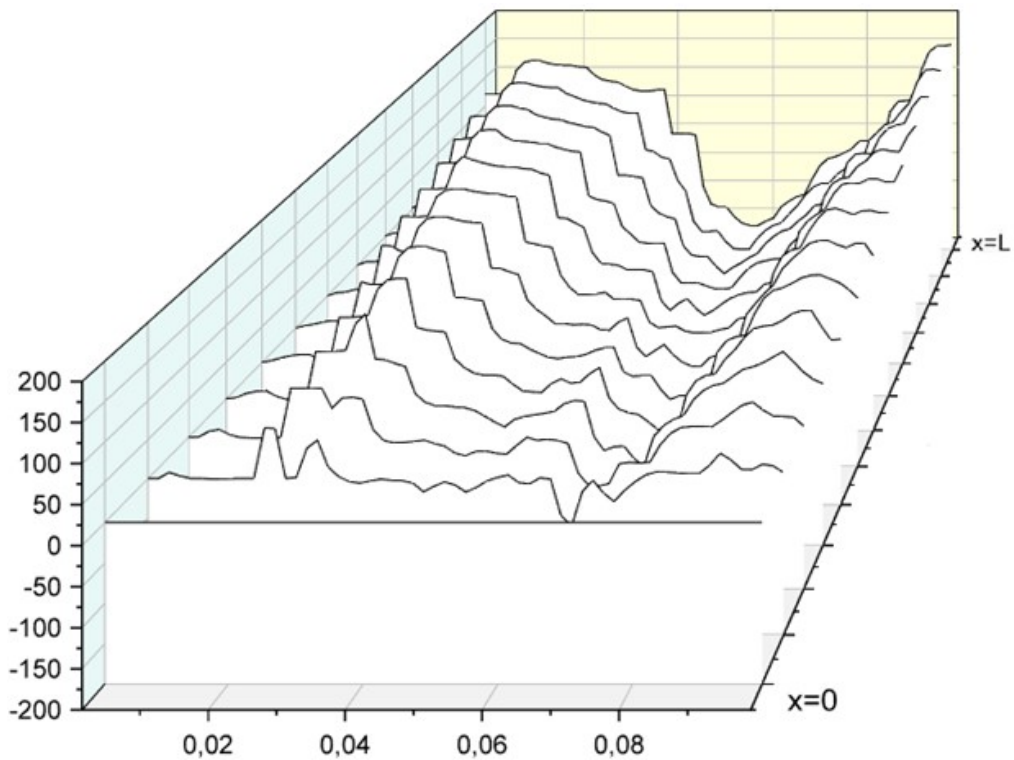


**Figure 8 – Results for different sections. Poisson and junction coupling. Pressure at valve for Delft Hydraulics Benchmark Problem A with free valve.**

## 4. CONCLUSIONS

The FSI four equation model has been implemented. The agreement obtained between exactly solution results and simulation is good. This fact indicates that FSI\_01 code is able to reproduce the main effects of Fluid-structure Interaction during hydraulic transients in a pipe conveying fluids, that is, friction Poisson and Junction couplings. For future work the author suggests the implementation of the eight [5] and the fourteen [2] equations models.

## ACKNOWLEDGMENTS

The authors would like to thank the Nuclear and Energy Research institute of the National Nuclear Commission (IPEN/CNEN) and the Brazilian Navy for the support during the research and development of this work.

## REFERENCES

1. C. S. W. Lavooij and A. S. Tijsseling, “Fluid-Structure Interaction in Liquid Filled Piping Systems,” *Journal of Fluids and Structures*, **5**, pp.573-595 (1991).
2. “Fluid transients and fluid-structure interaction in flexible liquid-filled piping”, [https://www.win.tue.nl/~atijssel/pdf\\_files/Wiggert-Tijsseling\\_2001.pdf](https://www.win.tue.nl/~atijssel/pdf_files/Wiggert-Tijsseling_2001.pdf) (2001).
3. A.S. Tijsseling, “Fluid-Structure Interaction in Liquid-Filled Pipe Systems: a Review,” *Journal of Fluids and Structures*, **10**, pp.109-146 (1996).
4. J. P. Tullis, *Hydraulics of pipelines: pumps, valves, cavitation, transients*, John Wiley & Sons, 1989.
5. R. G. ROCHA, “Fluid-Structure Interaction in Piping Systems conveying Liquids via Glimm Method,” 2011. 97 p. Doctorate thesis (Mechanical Engineering) – Universidade Federal Fluminense, UFF/RJ.
6. A. S Tijsseling, “Exact solution of linear hyperbolic four-equation system in axial liquid-pipe vibration,” *Journal of Fluids and Structures*, **18**, pp.179–196 (2003).
7. S. Li, B. W. Karney, G. Liu, “FSI research in pipeline systems – A review of the literature,” *Journal of Fluids and Structures*, **57**, pp.277–297 (2015).
8. D. Ferras, P. A. Manso, A. J. Schleiss, D. I. C. Covas, “One-Dimensional Fluid-Structure Interaction Models in Pressurized Fluid-Filled Pipes: A Review,” *Applied Sciences(Acoustics and Vibrations)*, **8**, 1844 (2018).
9. A. S. Tijsseling’, “An overview of fluid-structure interaction experiments in single-elbow pipe systems” *Journal of Zhejiang University-SCIENCE A (Applied Physics & Engineering)*, **20**, pp. 233-242 (2019).
10. L. Zhang, A. S. Tijsseling, and A. E. Vardy, “FSI Analysis of Liquid- Filled Pipes,” *Journal of Sound and Vibration*, **224(1)**, pp.69-99 (1999).
11. S. Li, Y. Chen, C. Wang, “FSI Vibration Analysis Method of Complex Fluid-Filled Piping Systems,” *INTER-NOISE and NOISE-CON Congress and Conference Proceedings*, Chicago, IL, 26-29 august, pages 1 - 993, pp. 538-543(6), (2018).